This document is confidential and is proprietary to the American Chemical Society and its authors. Do not copy or disclose without written permission. If you have received this item in error, notify the sender and delete all copies.

A molecular theory of polypeptide adsorption at inorganic surfaces

Journal:	The Journal of Physical Chemistry
Manuscript ID	jp-2022-06607r.R2
Manuscript Type:	Special Issue Article
Date Submitted by the Author:	n/a
Complete List of Authors:	Gallegos, Alejandro; University of California Riverside, Department of Chemical and Environmental Engineering Wu, Jianzhong; University of California Riverside, Department of Chemical and Environmental Engineering

SCHOLARONE™ Manuscripts

A Molecular Theory of Polypeptide Adsorption at Inorganic Surfaces

Alejandro Gallegos and Jianzhong Wu*

Department of Chemical and Environmental Engineering, University of California, Riverside,

CA 92521, USA

Abstract

A faithful description of polypeptide adsorption at ionizable surfaces remains a theoretical challenge from a molecular perspective due to the strong coupling of local thermodynamic non-ideality and ionizations of both the adsorbate and substrate that are sensitive to the solution condition such as pH, ion valence, and salt concentration. Building upon a recently developed coarse-grained model for natural amino acids in bulk electrolyte solutions, here we report a molecular theory applicable to polypeptide adsorption on ionizable inorganic surfaces over a broad range of inhomogeneous conditions. Our thermodynamic model is able to account for the effects of the amino-acid sequence as well as surface association such as hydrogen bonding or bidentate coordination regardless of the solution pH, salt type and concentration. The theoretical predictions have been validated by extensive comparison with experimental data for the adsorption isotherms of three representative polypeptides at a titanium surface.

Keywords:

Surface adhesion, adsorption, charge regulation, Ising density functional theory

^{*} Corresponding author. E-mail addresses: jwu@engr.ucr.edu

1. Introduction

Understanding the thermodynamic properties of polypeptides at interface is of critical importance to a myriad of real-world problems and technological applications such as surface fouling in biomedical devices and food systems¹⁻³, adhesion in wet environments^{4,5}, and controlled drug delivery⁶⁻⁸. A theoretical description of polypeptides is complicated because of the diversity in amino-acid sequences and the flexibility in the microscopic structure and charge behavior sensitive to the local environment. Under inhomogeneous conditions, each amino-acid residue exhibits unique interactions with other residues and chemical species in the solution as well as with the interface. To account for the sequence effect, a theoretical model must distinguish segment-level interactions including different charge states of ionizable residues. For adsorption at an inorganic surface, the model must incorporate possible ionization of the substrate and the inherent coupling between the chemical equilibrium and local ionic distributions. To complicate the matter further, the charge behavior of both the polypeptide and the surface is sensitive to the solution conditions such as pH, ion valence, and salt concentration.

Experimental investigations of polypeptides at interface provide a useful guide in the development of a satisfactory thermodynamic model. In particular, a wide variety of techniques have been used to study the interfacial behavior of polypeptides at inorganic surfaces^{9, 10}. For example, phage display¹¹, quartz crystal microbalance measurement¹², ellipsometry¹³, and surface plasmon resonance (SPR)¹⁴ are a few methods that are commonly used to determine the affinity of polypeptides binding with specific surfaces. Alternatively, single molecule force spectroscopy (SFMS) provides insight about the interaction between polypeptides and an inorganic surface at the single-molecule level, thereby allowing for a detailed study of molecular interactions not available with other techniques¹⁵. Maity et al. took advantage of SFMS to identify the amino-acid

sequence effect by replacing a proline residue in a polypeptide chain with an alanine residue and found that the mutation had a detrimental impact on the binding capability with a mica surface¹⁶. The reduced binding was attributed to differences in the conformational freedom of the polypeptide when the residue was changed from proline to alanine. The distinctive cyclic structure of the proline residue leads to a high conformational rigidity in the polypeptide chain compared to that with the alanine residue. The experimental results thus unequivocally demonstrate the importance of segment-level details in determining polypeptide adsorption. The importance of intramolecular interactions in polypeptides and the resulting multibody correlations makes polypeptide adsorption distinctively different from their monomeric counterparts (viz. amino acids). Another technique that is commonly utilized to evaluate the affinity of peptides with inorganic surfaces is through peptide arrays. The combinatory procedure provides a quick evaluation of the surface affinity by measuring the change in the color of the solution due to the peptide binding¹⁷. The resulting color changes can then be mapped into binding scores to unravel the mechanisms underlying the adsorption (or lack thereof) of the polypeptide to the surface.

The interfacial behavior of polypeptides can also be measured indirectly by monitoring its concentration in the bulk phase upon interacting with a surface. The adsorption isotherm, i.e., the amount of polypeptide attached to the surface as a function of the *equilibrium* concentration in the bulk solution, can be determined from the reduction of the polypeptide concentration in the bulk solution¹⁸⁻²³. By utilizing semi-empirical models such as the Langmuir equation, one can gain valuable insight into the strength of surface binding. Unfortunately, semi-empirical models often have little predictive capability. They are mostly used only as a benchmark for comparing different polypeptides as well as different surfaces and solution conditions. Nevertheless, the experimental adsorption data are valuable for the calibration of various thermodynamic models and validation

of their hypotheses to account for the key physics necessary to describe different aspects of surface-polypeptide interactions.

A number of theoretical methods have been proposed to describe the adsorption and interfacial behavior of polypeptides at inorganic surfaces^{24, 25} ²⁶. These methods offer valuable insights to bridge the knowledge gap between microscopic and macroscopic observations. For example, Kurut et al. utilized molecular simulation and a polymer density functional theory (DFT) to study the charge regulation of histidine in unstructured peptides at interfaces²⁷. They found that the adsorption of the peptide composed of histidine to be weaker at pH 8 than 6 because the histidine residues are less likely to be charged. In addition, added salt lowered the adsorption amount due to the screening effect on electrostatic-driven adsorption. Biesheuvel et al. studied the adsorption of ionizable polyelectrolytes such as lysozyme on a silica surface using a modified Poisson-Boltzmann model²⁸. The mean-field method accounted for charge regulation due to intermolecular electrostatic interactions between the surface, ions, and ionizable proteins. In general, the adsorption of lysozyme exhibited a maximum in adsorption with pH at a pH less than the isoelectric point. The increase in the salt concentration reduced the adsorption at high pH when the adsorption was electrostatic-driven, whereas the added salt would increase the adsorption at low pH when the electrostatic interactions between the surface and the lysozyme were less important. A different approach by Leermakers et al. utilized a polymer self-consistent-field theory to study the adsorption of β -Casein^{29, 30}. They found that the protein formed a dense layer near the surface and that the adsorption tended to increase with pH and bulk protein concentration.

Molecular simulation methods have also been utilized for predicting polypeptide adsorption with different levels of microscopic details, ranging from atomistic to coarse-grained models. For example, Verde et al. employed an all-atom molecular dynamics (MD) simulation to

study peptide adsorption on a gold surface³¹. It was found that the dynamics of peptide adsorption is dictated by a free-energy barrier that depends on the chain flexibility. The key to overcoming the barrier to adsorption was that the peptide must have high conformational flexibility but low conformational stability, i.e., the polypeptide should be able to freely adapt to the surface/local environment and does not get trapped in a single conformation. Xie et al. investigated the adsorption of neuromedin-B peptide, a decapeptide originally isolated from porcine spinal cord, at different self-assembled monolayers (SAM) using all-atom MD simulation³². They found that the surface induces the peptide conformational change compared to that in the bulk solution and that the variation was greatest for a hydrophobic SAM. Alternatively, polypeptide adsorption has been investigated with coarse-grained models^{33, 34}. In comparison with atomistic methods, a coarsegrained model offers a significant decrease in the computational burden thus is suitable for the systematic study of more realistic systems. Hyltegren et al. investigated the adsorption of the saliva protein histatin 5 (24 residues) on silica surface using a bead-spring model with each bead representing an amino-acid residue³⁵. Their work highlights the importance of the peptide and surface charge in predicting the peptide adsorption. Further details can be included in the coarsegrained description of polypeptide adsorption. For example, Qiu et al. used the Martini model that maps each residue into one or more beads in order to capture its intrinsic characteristics such as polarity and shape.³⁶ They identified the important role of the adsorbed water in driving the polypeptide adsorption to a neutral surface through van der Waals forces.

A major difficulty in modeling polypeptide adsorption lies in the accurate representation of solution conditions (e.g., pH, ion valence, and salt concentration). The environmental effects are important not only for polymer-surface interactions but also for both the inter- and intramolecular interactions that dictate the peptide conformation. In particular, the solution

condition directly influences the charge behavior of the polypeptide and substrate that is often utilized for the dynamic control of the polypeptide properties in practical applications. Recently, Grünewald et al. demonstrated a convenient way to incorporate titratable beads into the Martini coarse-grained model³⁷. Conversely, the charge regulation can be implemented with thermodynamic models that explicitly take into account ionization equilibrium. The theoretical calculations are significantly faster than the simulation counterparts. One example of the theoretical approach is by incorporating charge regulation through the mean-field approximation, i.e., the average ionization of each monomer or surface site is assumed uncorrelated with other ionizable groups in the system³⁸. The mean-field approximation allows for the consideration of multi-chain systems near ionizable surfaces under realistic conditions, opening up the possibility of computational screening and materials design^{10, 39, 40}. A similar mean-field approach to charge regulation was used in the work by Kurut et al. discussed earlier²⁷. Typically, the mean-field methods fail to account for the influence of intramolecular correlations on the ionization behavior of individual residues.

In a previous work,⁴¹ we developed a coarse-grained model for describing the adsorption of natural amino acids onto inorganic surfaces in various aqueous solutions. The thermodynamic model provides a faithful description of the charge behavior of the amino acids as a function of pH and solution conditions. We demonstrated that the charge regulation of various ionizable surfaces is well described by an explicit consideration of the inhomogeneous ion distributions and protonation/deprotonation reactions⁴². Herein, we extend the coarse-grained model to polypeptides and examine their adsorption behavior at the titanium surface leveraging on the recently developed Ising density functional theory (iDFT)⁴³. The molecular thermodynamic model allows us to predict the adsorption of various polypeptides in response to the changes in solution

conditions. The predictive molecular theory fills the gap between phenomenological models to describe polypeptide adsorption and various molecular simulation methods. Importantly, the theoretical procedure opens new possibilities for the future studies of polypeptide systems including polymer-mediated adhesion.

2. Thermodynamic Model and Methods

2.1 A coarse-grained model for polypeptide adsorption

In this work, we are interested in developing a generic model applicable to polypeptide adsorption at ionizable surfaces over a broad range of solution conditions. Toward that goal, we employ an augmented primitive model (APM) that takes into account the molecular excluded volume effects, short-ranged solvent-mediated interactions, and different ionization states of each amino-acid residue as well various ionizable functional groups at the surface. In APM, each monomer or polymer segment has a unique hard-sphere diameter σ_i , and may exist in different charge states as described by the "Ising parameter" s_i . Except the chain connectivity, the coarse-grained model is similar to our previous studies for the adsorption of amino acids and their titration behavior in bulk solutions^{41, 44}. The equilibrium constant for the ionization of each amino acid side chain is assumed to be the same as that for the monomer⁴⁴.

Figure 1 shows a schematic representation of a polypeptide chain near an inorganic surface as described by our coarse-grained model. We describe polypeptides as tangent-hard-sphere chains in which each monomer represents one amino-acid residue. These monomers can be acidic, basic, or neutral depending on the functional groups in the side chain and the charge of the monomer is dependent on the local environment. In addition, we consider the end-effects (viz. the C- and N-terminus groups) in the polypeptide chains where the -NH₂ and -OH groups are described as ionizable hard spheres ($\sigma_{NH_3/OH} = 3.0 \text{ Å}$). The equilibrium constants for the terminus groups

correspond to the previously determined values for the natural amino acids⁴⁴. In the absence of polypeptides and ionizable surface, the coarse-grained model reduces to the conventional primitive model of aqueous electrolyte solutions, i.e., the ions are represented by charged hard spheres and the solvent by a dielectric continuum of relative permittivity $\varepsilon_r = 78$, which corresponds to that for liquid water at ambient conditions. The augmented aspect of the primitive model refers to, in part, the consideration of ionization equilibrium for each amino-acid residue and the inclusion of various well-recognized but poorly understood water-mediated interactions. For simplicity, we assume that such interactions are short-ranged and can be empirically represented through the square-well (SW) model. Throughout this work, the SW width is fixed at $\delta_{surf} = 0.4 \, \text{nm}$, approximating the same as the diameter of a water molecule⁴⁵.

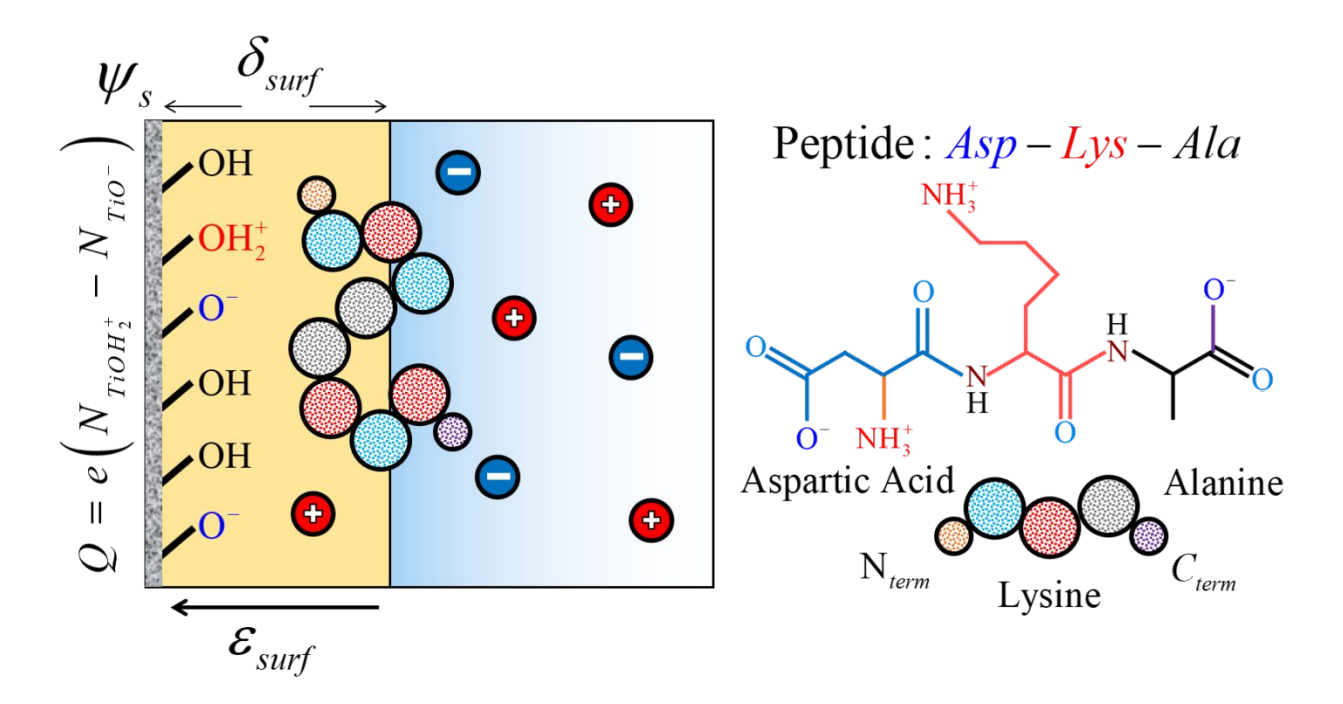


Figure 1. Schematic of a coarse-grained model for polypeptide adsorption on an ionizable surface.

A polypeptide molecule is represented by a tangent-hard-sphere chain such that each segment corresponds to an amino-acid residue and the N- and C-terminus groups are considered explicitly.

In addition to electrostatic interactions due to the charge of ionizable residues and the terminus

groups at the surface, amino-acid residues bind with the surface through chemical association and solvent-mediated interactions represented by a square-well potential of strength ε_{surf} and width δ_{surf} .

While the phenomenological model neglects atomic details and the anisotropic nature of individual residues, it provides a flexible framework to quantify the interfacial behavior of polypeptides by treating the square-well attraction energy ε_{surf} as an adjustable parameter. Approximately, this parameter characterizes the short-range interaction between an amino-acid with a specific surface thus may be assumed independent of the solution conditions. We demonstrated in our previous work that the augmented primitive model can well describe the thermodynamic properties of amino acids in bulk solutions as well as their adsorption to inorganic surfaces and the theoretical predictions were found in good agreement with experimental observations^{41,44}. Further details on the molecular model can be found in our previous work.

Polypeptide adsorption at an inorganic surface is driven by either electrostatic attraction or surface binding (non-electrostatic). While the electrostatic interactions are coupled with ionic species in the solution, we expect that the surface binding is relatively insensitive to solution conditions directly. The non-electrostatic potential is thus represented by a square-well model with a constant surface energy for each residue

$$V_{i}^{ext}(z) = \begin{cases} \infty & z < \sigma_{i} / 2 \\ -\varepsilon_{surf,i} & \sigma_{i} / 2 \le z \le \delta_{surf} \\ 0 & else \end{cases}$$
 (2)

Spruijt et al. proposed that the binding strength of polymers containing carbonyl groups to a silica surface is dependent upon the number of surface hydroxyl groups that are not deprotonated⁴⁶. Their reasoning follows from the fact that the hydrogen bonds between the surface hydroxyl group

and the carbonyl group cannot occur when the surface is deprotonated. The surface groups will deprotonate as the pH is increased, which results in fewer binding sites for the polymer thereby a weaker average binding energy. In this work, we also find that the attraction energy is related to the available surface sites (*viz.* surface functional groups) that the polymer can bind to and such effects can be represented by the empirical relation:

$$\varepsilon_{surf,i} = \varepsilon_{surf,i}^{0} \left[1 - \left(\frac{N_{TiO^{-}}}{N_{sites}} \right) \right] \left[1 + \left(\frac{N_{TiO^{-}}}{N_{sites}} \right) \right]$$
(3)

where $\varepsilon_{surf,i}^0$ is the surface binding energy at an uncharged surface, and N_{TiO^-}/N_{sites} corresponds to the fraction of negatively charged surface sites. The determined empirical relation indicates that the attractive binding energy will decrease with an increased presence of the negatively charged surface sites as one expects from the decrease in possible binding sites. However, there is a less than linear dependence of the binding energy on the fraction of negatively charged sites since the monomer can still interact with nearby sites that surround it. Within our model, there is no difference in the interaction energy between a neutral site and a positively charged site. In reality, the protonated site $(-TiOH_2^+)$ may have a slightly stronger hydrogen bond energy than the neutral site (-TiOH).

In addition to physical interactions, we also consider the charge regulation of the inorganic surface through the deprotonation and protonation of the surface hydroxyl sites. For the titanium dioxide surface considered in this work, the deprotonation and protonation reactions are given by

$$-TiOH \rightarrow -TiO^{-} + H^{+}, \tag{4}$$

$$-TiOH+H^{+} \rightarrow -TiOH_{2}^{+}. \tag{5}$$

These reactions are governed by the equilibrium constants, K_D and K_P , respectively, which are related to the solution pH = $-\log a_{H^+}$ and the activities of the surface sites:

$$K_D = \frac{N_{TiO^-}}{N_{TiOH}} \frac{\gamma_{TiO^-}}{\gamma_{TiOH}} a_{H^+}, \tag{6}$$

$$K_{P} = \frac{N_{TiOH_{2}^{+}}}{N_{TiOH}} \frac{\gamma_{TiOH_{2}^{+}}}{\gamma_{TiOH}} \frac{1}{a_{H^{+}}}, \tag{7}$$

where N_i refers to the number of surface site i per unit area, and γ_i is the activity coefficient of the corresponding surface site.

The activity coefficient of each surface group accounts for its physical interactions with the local environment⁴⁷. In this work, we assume that the surface activity coefficients are mainly determined by the electrostatic interactions between surface sites, ions, and the polypeptides. As a result, we can express the ratio of activity coefficients for the uncharged to charged states of the surface functional groups by the mean electrostatic potential (viz. $\gamma_{TiOH} / \gamma_{TiOH} = \exp[\beta e\psi_s]$ and $\gamma_{TiOH} / \gamma_{TiOH} = \exp[-\beta e\psi_s]$. The equilibrium constant and the ratio of activity coefficients can be combined into an *apparent* equilibrium constant: $K_D' = K_D \gamma_{TiOH} / \gamma_{TiOH}$ and $K_P' = K_P \gamma_{TiOH} / \gamma_{TiOH}$ which correspond to the experimentally measured equilibrium constants.

An explicit expression for the surface charge density can be derived in terms of the total number of available sites per unit area, the apparent equilibrium constants, and the proton activity a_{H^+} :

$$Q = -e\left(N_{TiO^{-}} - N_{TiOH_{2}^{+}}\right) = -e N_{sites} \frac{K_{D}' / a_{H^{+}} - K_{P}' a_{H^{+}}}{1 + K_{D}' / a_{H^{+}} + K_{P}' a_{H^{+}}}$$
(8)

where the total number of ionizable sites, $N_{sites} = N_{TiOH} + N_{TiO^-} + N_{TiOH_2^+}$, can be determined from experimental data or estimated from the crystalline structure. Since the surface charge is related to the mean electrostatic potential through Gauss' equation, there is a coupling between the surface

charge and the polypeptide adsorption. A comprehensive description of the surface charge regulation can be found in our previous publications^{41, 42}.

2.2 Ising Density Functional Theory

Ising density functional theory (iDFT) provides a convenient avenue to describe the ionization of weak polyelectrolytes at inhomogeneous conditions⁴³. For a polypeptide represented by M ionizable segments, the chain conformation is fully specified by a multidimensional vector, $\mathbf{R} = (\mathbf{r}_1, \mathbf{r}_2, ..., \mathbf{r}_M)$, where \mathbf{r}_i denotes the segment position, and the ionization state of the entire polymer chain can be specified by vector $\mathbf{S}_k = (s_1, s_2, ..., s_M)$, where $s_i = \pm 1$ or 0 is the charge number (viz., the valence of segment i in the polypeptide chain). In the context of polypeptide adsorption, the density profile in configuration $\mathbf{X} = (\mathbf{R}, \mathbf{S})$ is given by

$$\rho(\mathbf{X}) = \exp\left\{-\beta[V^{B}(\mathbf{X}) + V^{ext}(\mathbf{X}) + \mu^{ex}(\mathbf{X}) + \mu^{\infty}(\mathbf{X}) + \mu^{H}(\mathbf{S}) - \mu]\right\}$$
(9)

where $V^B(\mathbf{X})$ represents the bond potential, μ is the chemical potential of the polypeptide in its fully uncharged state, V^{ext} is the non-electrostatic external potential for the entire chain (that for each segment is given by Eq. 1), $\mu^{ex}(\mathbf{X}) = \delta F^{ex} / \delta \rho(\mathbf{X})$ is the local excess chemical potential to account for the thermodynamic non-ideality due to inter- and intra-molecular interactions, $\mu^{\infty}(\mathbf{X})$ is the contribution to the potential energy due to the intramolecular electrostatic interactions in configuration \mathbf{X} , and $\mu^H(\mathbf{S})$ is affiliated with the ionization of individual segments, i.e.,

$$\mu^{H}(\mathbf{S}) = \sum_{i}^{M} \Delta \mu_{i}^{H} = -\ln 10 k_{B} T \sum_{i}^{M} s_{i} (pK_{i} - pH).$$
 (10)

The ionization energy accounts for the change in the grand potential due to deprotonation/protonation of the ionizable segments. The equilibrium constant of the ionization

reaction, K_i , depends on the identity of the ionizable site and system temperature but not on the solution composition.

According to the thermodynamic perturbation theory (TPT), the local excess chemical potential can be decomposed into one-body and two-body contributions:

$$\mu^{ex}(\mathbf{X}) = \sum \left[\mu_i^{mon}(\mathbf{x}_i) + \mu_i^{ch}(\mathbf{x}_i) \right] + \sum \ln y(\mathbf{x}_i, \mathbf{x}_{i+1})$$
(11)

where μ_i^{mon} is the excess chemical potential for the monomer system, μ_i^{ch} is excess chemical potential due to chain connectivity which describes the free energy due to intrachain correlation by segment i in state s_i , and $\ln y$ is the natural logarithm of the two-body cavity correlation function. The first summation accounts for the thermodynamic non-ideality due to monomeric interactions, and the second summation accounts for the intramolecular correlations⁴⁸. In this work, we consider the excluded-volume effects through the modified fundamental measure theory⁴⁹, the electrostatic correlations by the reference fluid method using the mean spherical approximation ⁵⁰, and the square-well attractions through a mean-field method⁴⁵.

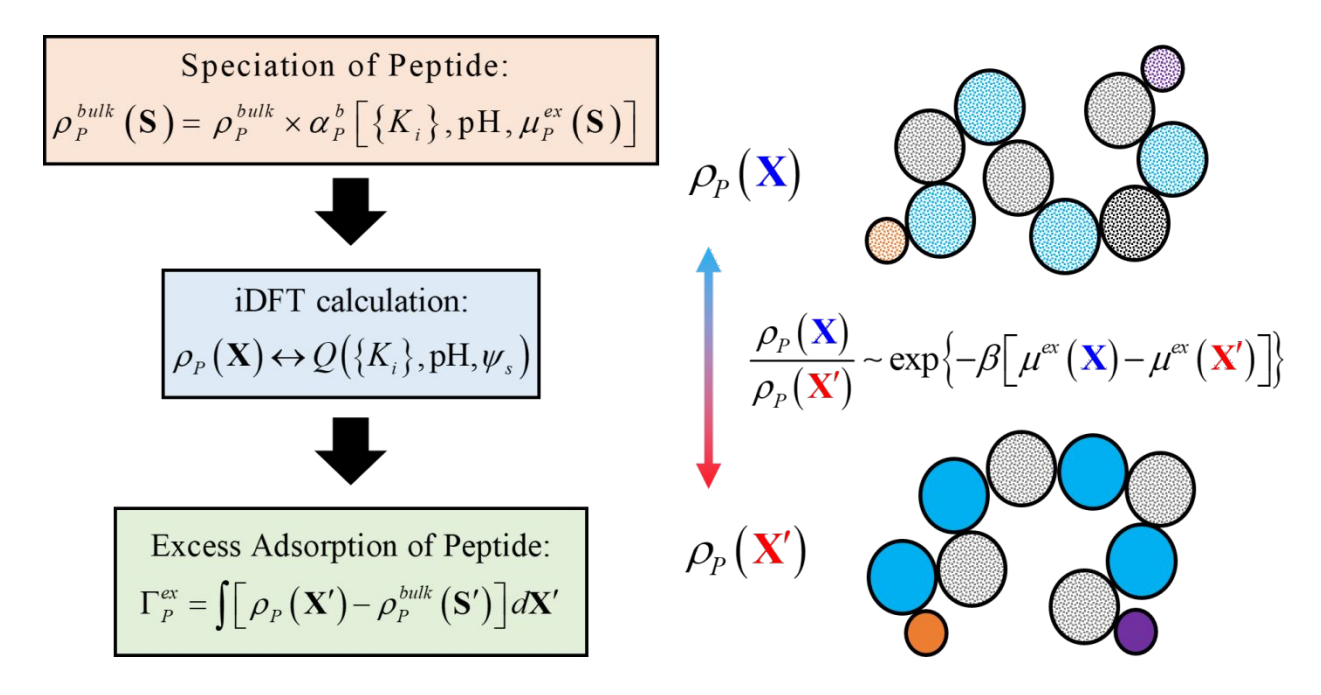


Figure 2. A flowchart for predicting the adsorption of peptides on an inorganic surface through the Ising density functional theory (iDFT).

Figure 2 presents a flowchart to determine the adsorption of polypeptides on an inorganic surface. In numerical implementation of iDFT, we first determine the speciation of the polypeptide in the bulk solution:

$$\rho_{P}^{bulk}\left(\mathbf{S}\right) = \rho_{P}^{bulk} \times \frac{\exp\left[-\beta\left\{\mu^{ex}(\mathbf{S}) + \mu^{\infty}\left(\mathbf{S}\right) + \mu^{H}(\mathbf{S})\right\}\right]}{\sum_{SS} \exp\left[-\beta\left\{\mu^{ex}(\mathbf{S}') + \mu^{\infty}\left(\mathbf{S}'\right) + \mu^{H}(\mathbf{S}')\right\}\right]}$$
(12)

where $\mu^{ex}(\mathbf{S})$ and $\mu^{\infty}(\mathbf{S})$ are the bulk counterparts of $\mu^{ex}(\mathbf{X})$ and $\mu^{\infty}(\mathbf{X})$, respectively. Eq.(11) follows from Eq.(8) by assuming that the segment densities are uniform and the inter- and intramolecular correlations are independent of the polymer conformation \mathbf{R} . Because the intramolecular interactions are evaluated at the nearest-neighbor level (i.e., interaction between i and i+1 only), we can solve Eq. (11) using a numerical procedure the same as that for the nearest-neighbor site-binding model of weak polyelectrolyte titration⁵¹. In the bulk solution, the inter- and intramolecular correlations are dependent upon the average concentrations of ions and polypeptide segments. Because the excess chemical potential of the polypeptide depends on its valence vector \mathbf{S} , the adsorption model must self-consistently account for the speciation of the polypeptide in the bulk.

Next, we solve for the density profiles of the polypeptide segments and salt ions near the inorganic surface. The polypeptide adsorption is coupled with surface ionization which depends on the local environment (viz. mean electrostatic potential). Different from alternative methods that consider only the intermolecular interactions on the inhomogeneous distributions of polypeptide chains and salt ions²⁸, iDFT takes into account the effects of intramolecular correlations on the polypeptide charge and chain conformation. The intrachain contribution is

particularly important for polypeptides with different types of charged residues in which the amino-acid sequence can play an important role in the adsorption behavior.

Lastly, we calculate the surface excess, i.e., the adsorption of individual amino-acid residues in their specific charge states from

$$\Gamma_{P,i}^{ex}(s_i) = \int \left[\rho_i(\mathbf{r}, s_i) - \rho_i^{bulk}(s_i) \right] d\mathbf{r}$$
(13)

where the density profile of each residue in its charge state is given by

$$\rho_i(\mathbf{r}, s_i) = \exp\left\{-\beta \left[V^{ext}(\mathbf{r}, s_i) + \mu_i^{mon}(\mathbf{r}, s_i) + \Delta \mu_i^H(s_i) - \mu\right]\right\} G_i^L(\mathbf{r}, s_i) G_i^R(\mathbf{r}, s_i). \tag{14}$$

In Eq.(13), G_i^L and G_i^R are the propagator functions that account for the possible configurations of the polymer given that segment i is at position \mathbf{r} in charge state s_i^{43} . Additional details on iDFT calculations can be found in our previous publication⁴³.

3. Results and Discussion

In our previous work, we demonstrated that classical density functional theory (cDFT) can well capture amino acid adsorption and the influence of pH and salt concentration on the ionization of natural amino acids in the bulk and near inorganic surfaces⁴². In the following, we provide 3 case studies to illustrate the application of our coarse-grained model to describe the pH effect on the adsorption of oligopeptides at a planar surface of titanium oxide. These oligopeptides are composed of some or all of the following amino-acid residues: alanine, lysine and aspartic acid. The equilibrium constants for two ionizable residues are taken from our previous work⁴⁴: $pK_{Lys} = 10.95$ and $pK_{Asp} = 3.97$. The experimental data used for the validation of our theoretical results are from Imamura et al.⁵². Unfortunately, no titration data were reported for the titanium

dioxide surface used in the experimental work for oligopeptide adsorption. To minimize unknown parameters, we adopted the equilibrium constants for protonation and deprotonation of the hydroxyl groups, $pK_p = -4.1$ and $pK_D = 6.5$, respectively, from a titanium surface different than the one considered in the experimental work⁴¹. We expect that the equilibrium constants should not differ from those of the surface studied by Imamura et al. Because differences in surface preparation could change the number density of the hydroxyl sites on the surface⁵³, we use the surface site density of 1.0 #/nm² to best fit the experimental data.

For comparison with the experimental adsorption isotherms, we determine a binding energy ($\varepsilon_i > 0$ is attractive) for each amino-acid residue based off correlation with the experimental data by Imamura et al.⁵² shown in the figures to follow: $\varepsilon_{surf,Asp}^0 = 5.50k_BT$, $\varepsilon_{surf,Asp}^0 = 3.75k_BT$, and $\varepsilon_{surf,Lys}^0 = 1.90k_BT$. The non-electrostatic binding energy is affiliated with the hydrogen bonding by the carbonyl group in the polypeptide backbone and an additional binding capability by the carboxyl group in aspartic acid. The energy values are weaker than that found for the adsorption of natural amino acids to titanium because of the absence of the amine and carboxyl groups in the residues (viz. loss in hydrogen bonding groups)⁴¹. The binding strength of lysine is lower than that of the alanine residue even though they both contain one carbonyl group. The difference may be indicative of the extended conformation of the lysine structure that favors the side chain orientation towards the surface and therefore, the backbone carbonyl group will be less likely to interact with the surface.

3.1 Adsorption of oligopeptide with acidic and neutral residues

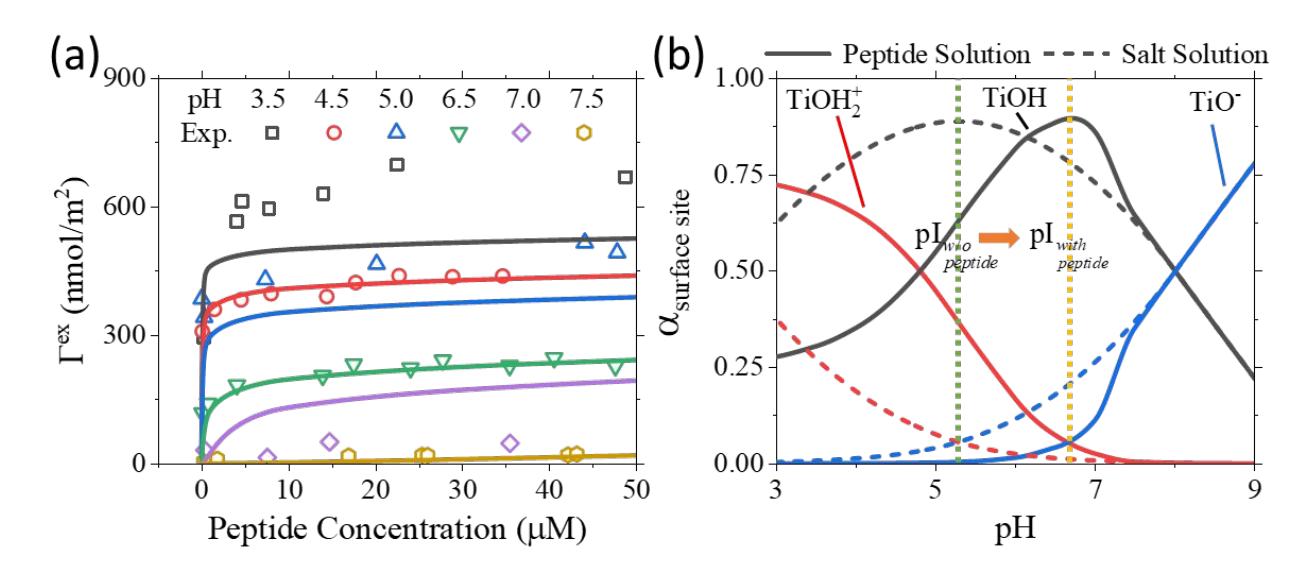


Figure 3. (a) Adsorption isotherms for polypeptide DADADADA on the titanium surface in a 100 mM potassium nitrate solution. The lines are the theoretical predictions and the symbols are experimental data⁵². (b) The fractions of ionizable sites on the titanium surface with and without the polypeptide (at 50 μ M) in 100 mM KNO₃ solution. The surface sites $TiOH_2^+$, TiOH, and TiO^- correspond to the red, black, and blue lines, respectively.

We first consider the adsorption of oligopeptide DADADADA on a titanium surface as investigated experimentally by Imamura et al.⁵². The peptide is composed of four acidic residues (viz. aspartic acid, D) and four neutral residues (viz. alanine, A). The adsorption isotherm is considered in the range of 0 to 50 μ M peptide concentrations at 6 pH values in a 100 mM potassium nitrate solution. Figure 3a shows a comparison between the theoretical and experimental results. In general, the decrease in pH results in an enhanced adsorption of the acidic polypeptide. The trend is expected because the oligopeptide is predominately negatively charged (due to the deprotonation of the carboxyl side chain in the aspartic acid residues) while the titanium surface increases in charge with a decrease in pH. The increased adsorption at low pH is thus driven by more favorable electrostatic interactions between the negatively charged polypeptide and the

positively charged surface. In addition, the adsorption is favored by the non-electrostatic surface binding as evidenced by the excess adsorption of the peptide at the surface up to pH 7.5 when the titanium surface is negatively charged (isoelectric point of 5.3)⁴¹. Overall, our theoretical predictions agree with the experimental results at a semi-quantitative level indicating that the coarse-grained model for polypeptide adsorption captures the ionizations of both the aspartic acid residues and the titanium surface reasonably well. The most noticeable discrepancy between our model and the experimental results is for the conditions of pH 3.0. We find that our model underestimates the adsorption of the polypeptide which may be due to the stronger non-electrostatic binding of the monomer to the protonated surface that is not accounted for through Eq. (2). There is also a deviation between the theoretical and experimental results at pH 7.0 since our model predicts a slightly later decrease in the adsorption of the polypeptide with pH; however, our model does capture the large drop in adsorption from pH 6.5 to 7.5.

Figure 3b shows the influence of the polypeptide adsorption on the dissociation of the surface hydroxyl sites at the titanium surface. Without the polypeptide, the surface is positively charged at pH below the isoelectric point (pI=5.3) and negatively charged at pH above the isoelectric point. In the presence of the polypeptide ($\rho_p^{bulk} = 50 \mu M$), the surface composition is significantly different, in particular at low pH. The large change in the composition of surface sites can be attributed to the strong attraction (both electrostatically and non-electrostatically) of the aspartic acid and alanine residues to the surface. The isoelectric point of the titanium surface is shifted from 5.3 to approximately 6.7 as shown by the vertical dotted lines in Figure 3b. The negatively charged residues in the polypeptide promote the presence of positively charged sites on the surface and inhibit the formation of negatively charged sites, thereby shifting the surface isoelectric point to a higher pH value. As the pH is further decreased, the favorable electrostatic

interaction between the surface and the aspartic acid residues leads to a larger positive surface charge compared to the salt only solution. At low pH, the aspartic-acid residues start to lose their negative charge, which explains why the surface does not dissociate to the $-TiOH_2^+$ group as quickly with a decrease in pH as it does at a slightly higher pH since there are less favorable charge-charge interactions. At high pH, there is no difference in the titration of the titanium surface whether the polypeptide is present or not in the bulk solution since the polypeptide will no longer adsorb on the surface. Thus, we see that the correct treatment of the thermodynamic non-ideality in the charge regulation of both the residues and the surface is important for an accurate description of polypeptide adsorption on inorganic surfaces.

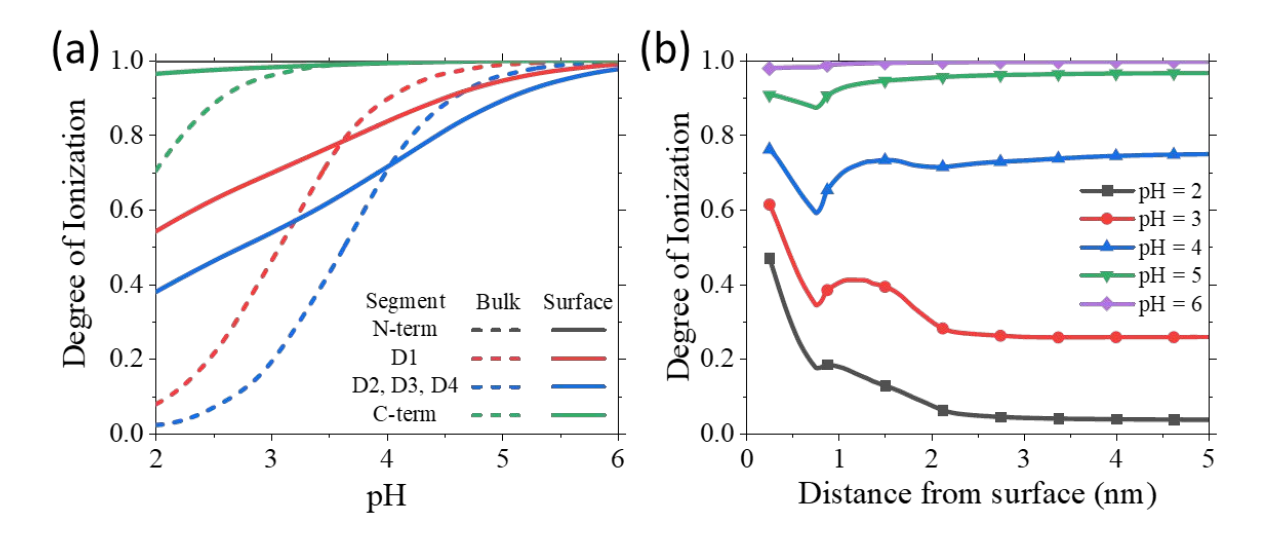


Figure 4. (a) The degree of ionization for aspartic-acid residues from DADADADA in the bulk and that adsorbed on the titanium surface. The lines for the middle residues, D2, D3, and D4, are nearly indistinguishable from one another and the lines for N-term are at $\alpha = 1.0$. (b) The average degree of ionization for aspartic-acid residues as a function of the distance from the surface for different pH values. In both panels, the peptide concentration is 50 μ M in the bulk and the bulk potassium chloride concentration is 100 mM.

The charge regulation of different amino-acid residues and terminal groups is key to the adsorption of the polypeptide to the titanium surface. We show in Figure 4a the degree of ionization for aspartic acid residues and the terminus groups in the bulk solution and adsorbed to the surface. As a result of the intrachain correlations and the spatial conformation of the polypeptide, the acidic residues may not necessarily be at the same average degree of ionization near the interface. We find that the ionization degree for the end residue (D1) is significantly greater than the degree of ionization for the middle residues (D2, D3, and D4) whether in the bulk or adsorbed at the surface. The similarity in the ionization for the three middle residues indicates that the intrachain correlations of the polypeptide play an important role in determining the charge status of these residues. While D2, D3, and D4 are surrounded by neutral alanine residues, D1 is neighbored by a positively charged N-terminus group (which is always charged below pH 9 as shown in Figure 4a); the ionization of the terminal residue (D1) is promoted by the favorable charge-charge interaction. Since the adsorbed polypeptides mostly lay flat on the surface, there is not a significant difference between the three aspartic-acid residues in the middle. A mean-field method (i.e., one that does not incorporate intramolecular interactions such as the modified Poisson Boltzmann method²⁸) would miss the different ionization behavior of aspartic acid residues at the end and in the middle.

The ionization of polypeptides near the interface is different from that in the bulk due to the changes in the local environment as well as the surface-induced interactions (i.e., charge regulation). At high pH, the polypeptide charge is unaffected by its local environment due to the strong chemical driving force. As the pH is reduced, the degree of ionization for the amino-acid residues at the surface is initially lower than that in the bulk solution. Since there is a strong adsorption of the polypeptide even when the surface is nearly neutral (~ pH 5), the repulsion

between charged aspartic-acid residues at the surface leads to the ionization of the residue being less favorable than that in the dilute bulk solution. However, as the pH is further decreased, the surface becomes sufficiently charged and results in a favorable electrostatic attraction that overcomes the mutual repulsion between the aspartic acid residues. In this case, the average ionization of the residues at the surface decreases slower with pH compared to the residues when they are in the bulk solution. Our theoretical method improves upon conventional approaches by capturing the charge regulation of the polypeptides due to both inter- and intra-chain correlations important for describing polypeptide adsorption on ionizable surfaces.

Figure 4b shows the average degree of ionization for the aspartic acid residues as a function of distance from the surface. When the polypeptide is distributed greater than 3 nm from the surface, its ionization behavior is almost identical to that in the bulk because the surface effects are negligible (i.e., salt ions have sufficiently screened the long-range electrostatic interaction). At short distances (i.e., within square-well width), the ionization of aspartic-acid residues is typically higher than that in the bulk due to favorable electrostatic interaction with the surface. For example, at pH 2 about half of the absorbed aspartic residues are charged due to interactions with the titanium surface, whereas aspartic-acid residues in the bulk solution are essentially neutral. Interestingly, within the surface region, there is a significant drop in the ionization between those residues in direct contact with the surface and those at the edge of the square-well potential. We attribute the large variation in ionization within the short distance to the strong screening of the positively charged surface sites by the large local concentration of negatively charged asparticacid residues. At low pH, the surface charge is not fully compensated by the oppositely charged amino-acid residues, and therefore, an increased presence of counterions near the surface explains the gradual decrease in ionization until it reaches that of the bulk. On the other hand, at higher pH

such as pH 4, the degree of ionization for polypeptides near the surface is lower than that in the bulk because the electrostatic repulsion among aspartic-acid residues becomes stronger than the surface attraction. In other words, electrostatic interactions with the oppositely charged surface becomes insufficient to compensate the repulsion among aspartic-acid residues accumulated at the surface.

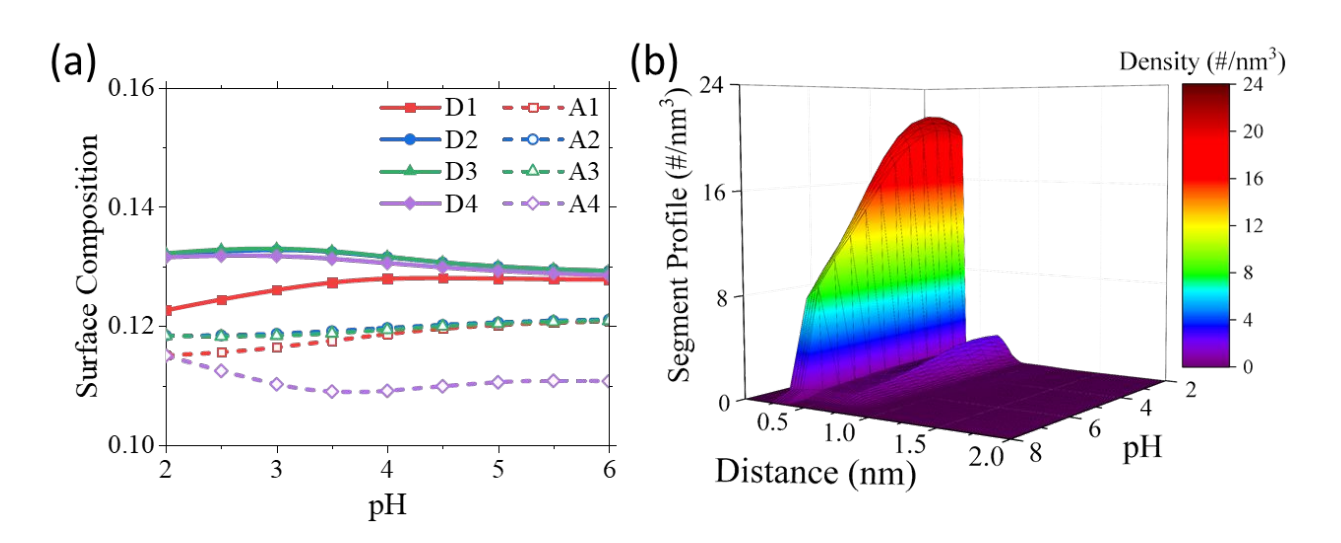


Figure 5. (a) The surface composition (defined by the fraction of species within a distance smaller than the square-well width) of different residues in oligopeptide DADADADA as a function of pH in a 100 mM KNO₃ solution. (b) The segment profile of the oligopeptide as a function of distance from the surface and the solution pH. The concentration of polypeptide and KNO₃ in the bulk are $50 \mu M$ and 100 mM KNO_3 , respectively.

We next investigate the polypeptide composition at the surface as defined by the fractions of different residues within a distance smaller than the square-well width. As shown in Figure 5a, the aspartic-acid residues are present at the surface to a higher degree than alanine residues. The difference can be attributed to higher non-electrostatic binding energy and to the favorable electrostatic interaction between the aspartic-acid residues and the surface. Nonetheless, the high presence of alanine residues within the surface region indicates that the polypeptides mostly lay

flat upon adsorption. Interestingly, the aspartic-acid residue on the N-terminus side of the oligopeptide, D1, is present at a lesser degree compared to the other three aspartic acid residues (D2, D3, D4), despite its higher degree of ionization. A similar behavior is found for the A4 residue which is connected to the C-terminus group. The reduction in the end-segment densities may be attributed to the depletion of the C- and N-terminus groups from the surface (their surface compositions are less than 0.02). Clearly, the explicit consideration of N- and C-terminus groups within our model has a significant influence on the adsorption of the neighboring residues in the polypeptide chain. Specifically, when the surface is positively charged (at low pH), the positively charged N-terminus groups are repelled from the surface thus reduce the adsorption of the neighboring aspartic-acid residue (D1). As the pH increases, the difference in the surface composition between residue D1 and the middle residues is negligible at pH greater than 6 because the surface is mostly neutral. In that case, the presence of the N-terminus group is no longer relevant. On the other end, the C-terminus group is negatively charged, and therefore it is attracted to the positively charged surface at low pH. However, the C-terminus group must also compete with the aspartic-acid residues for the electrostatic surface attraction. Besides, the A4 residue is located further from the surface than the middle alanine residues. Owing to intrachain correlations and electrostatic interactions with the surface, the inclusion of the terminus groups is an important component in understanding the conformation of polypeptides at ionizable interfaces.

Figure 5b shows the total segment distribution as a function of distance from the surface and pH. We see a noticeable increase in the polypeptide density at the surface as the pH is decreased, which follows from the adsorption trend as shown in Figure 3a. The polypeptide is adsorbed at the surface mostly due to the non-electrostatic binding energy. Beyond the square-well width, there is a sharp drop off in the segment density. The formation of a second peak in the

density profile arises from the excluded-volume effects and becomes more noticeable as the pH is decreased. The second peak may also be attributed to segments (mostly alanine) that are pushed out of the surface layer in favor of the adsorption of more aspartic-acid residues. The surface excess essentially disappears beyond the region of square-well attraction, suggesting that electrostatics alone is insufficient for the adsorption of polypeptides.

3.2 Adsorption of oligopeptides with basic and neutral residues

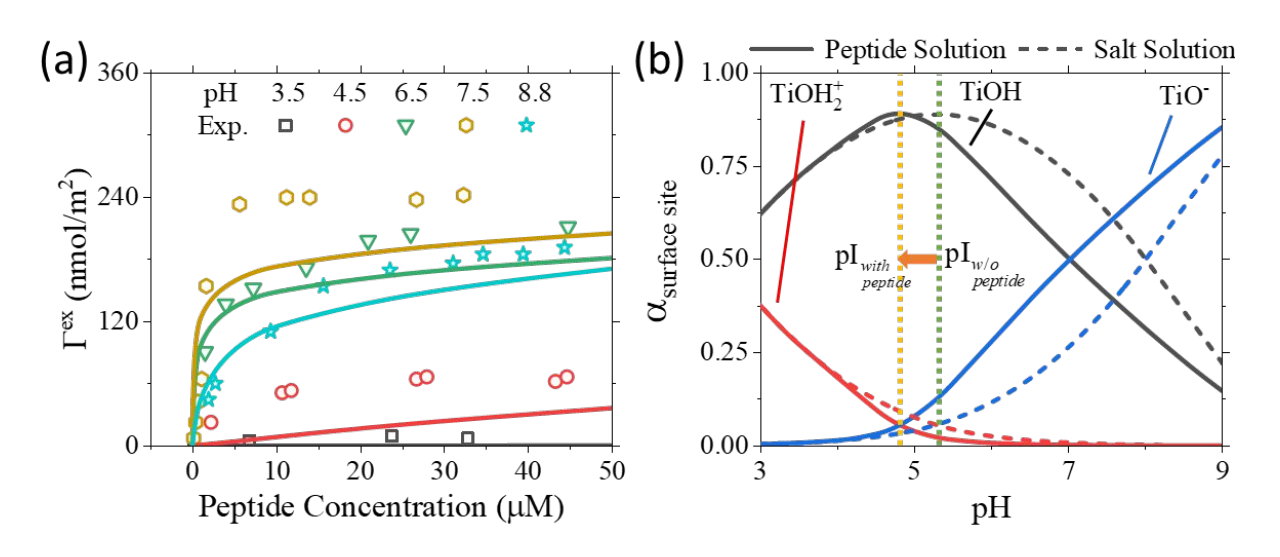


Figure 6. (a) The pH-dependence of adsorption isotherms for polypeptide KAKAKAKA on a titanium surface in a 100 mM potassium nitrate solution. The lines are theoretical predictions and the symbols are from experiment⁵². (b) The fractions of ionizable sites at the titanium surface in 100 mM KNO₃ solution with and without the polypeptide (at 50 μ M).

We next consider the adsorption of polypeptide KAKAKAKA to the titanium surface. The polypeptide is composed of four lysine residues and four alanine residues; the basic residues are fully ionized in the pH range considered in this work ($pK_{Lys} = 10.95$). As shown in Figure 6a, the polypeptide interacts favorably with the surface when it is negatively charged. The binding energies due to non-electrostatic interactions of the basic residues with the surface is much weaker than those of the acidic residues (viz., 1.90 k_BT vs. 5.50 k_BT), which leads to less adsorption

compared to the acidic polypeptide (see Figure 3a). Interestingly, the polypeptide adsorption increases with pH up to a maximum at pH 7.5 before decreasing as shown by the experimental results for pH 8.8. It would be expected that the adsorption of the basic polypeptide would continue to increase as the surface becomes more negatively charged (i.e., an increase in pH) since there are favorable charge-charge interactions and lysine residues maintain their positive charge even at pH>10. To explain the decrease in polypeptide adsorption, we focus our attention on the non-electrostatic interaction between the surface and the carbonyl group which is facilitated by a hydrogen bond to the surface -TiOH group (viz., we model this interaction through the squarewell potential). When the surface deprotonates, the peptide can no longer form hydrogen bond with the surface and therefore it loses its chemical binding capability. We model the loss in hydrogen bond capability through Eq.(2) by decreasing the binding energy as the surface hydroxyl sites deprotonate.. As a result, it becomes less favorable for the peptide to adsorb to the surface at high pH (viz. a decrease in the adsorption) since the adsorption is now facilitated mostly through the electrostatic interaction between the positively charged monomers and the negatively charged surface sites. Our model generally underestimates the adsorption of the basic polypeptide which may be attributed to the extended nature of the lysine residue that in reality allows for an increased likelihood of favorable interactions with the surface. While our model captures many of the important characteristics of polypeptides through its segment-level detail, it underestimates the conformational freedom of residues that can be significantly extended away from the overall polymer backbone.

Figure 6b shows the effect of polypeptide KAKAKA adsorption on the speciation of the titanium surface. Similar to the findings for polypeptide DADADADA, the speciation of the titanium surface is influenced by the polypeptide adsorption; although to a lesser degree since the

binding energy due to non-electrostatic interactions is much weaker (viz., 1.90 k_BT vs. 5.50 k_BT). There is a shift in the isoelectric point from 5.3 to 4.8 since the positively charged residues promote the deprotonation of the surface hydroxyl groups and inhibit the protonation. Since the polypeptide adsorption takes place in the pH range from 6 to 10, the surface behaves as it would in a solution without the polypeptide outside this pH range. As expected, the surface carries a greater negative charge at pH 7 when the peptide is adsorbed than it would have in the salt-only solution. Overall, our model performs well to capture the adsorption of the basic polypeptide to the titanium surface since we account for the change in non-electrostatic binding resulting from the loss in possible binding sites on the surface.

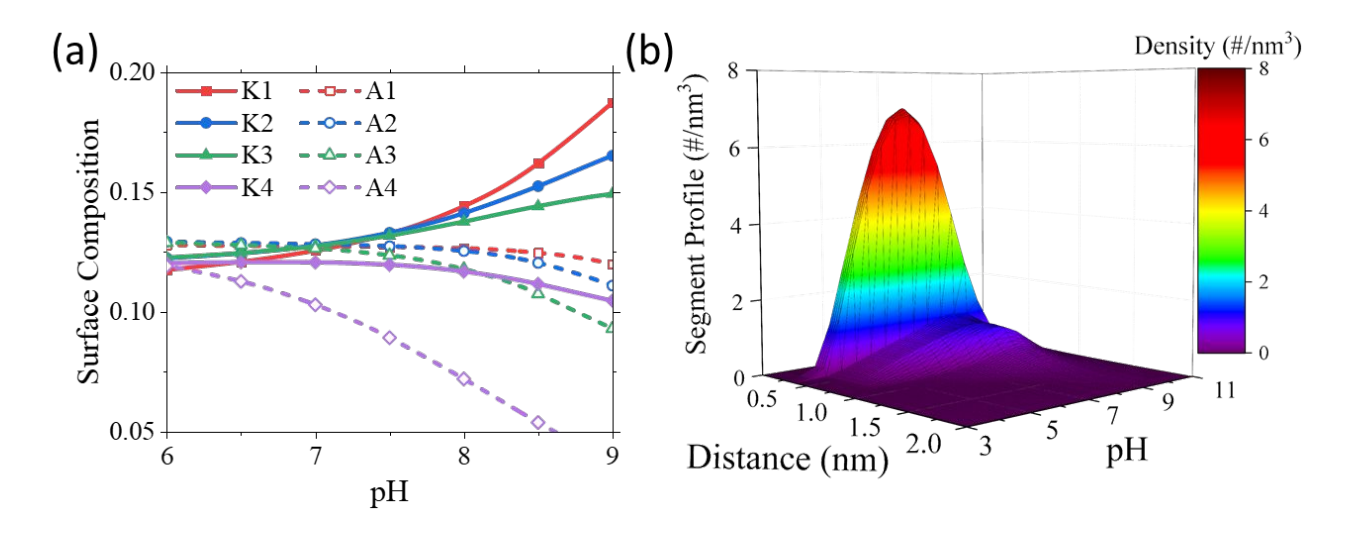


Figure 7. (a) The surface composition (defined as the fraction of residues within the square-well width) for the adsorption of oligopeptide KAKAKAKA as a function of pH. (b) The density profile of oligopeptide segments as a function of the distance from the surface and solution pH. The bulk concentrations of polypeptides and KNO₃ are 50 μ M and 100 mM, respectively.

Figure 7a shows the surface composition of oligopeptide KAKAKA adsorption at different pH values. Unlike the surface composition for the oligopeptide DADADADA, there is significant variation in the surface composition for the basic polypeptide in the segment

distribution with pH. The greater change can be attributed to the fact that the basic polypeptide does not interact with the surface non-electrostatically as strongly as the acidic polypeptide so it is more sensitive to the dependence of the surface charge on pH. In other words, the electrostatics plays a greater role in determining the conformation of basic KAKAKA polypeptide than the acidic DADADADA polypepetide. As the pH increases, K1 and A1 are the most likely to be present at the surface out of the other lysine and alanine residues, respectively. We can attribute this trend to the N-terminus group, which is positively charged in the pH range considered, and neighbors the K1 residue leading to two consecutive positive charges in the polymer chain that can interact favorably with the negatively charged surface. Since the A1 residue neighbors with the K1 residue, which in close contact with the surface, it is less likely for the A1 residue to orient away from the surface since K2 would also prefer to be near the surface. On the other end, the lysine residue K4 is followed by the neutral A4 residue and then the negatively charged C-terminus group. The C-terminus is repulsed by the negatively charged surface and therefore prefers to orient away from the surface. In addition, the A4 residue can bind non-electrostatically to the surface, but it is outcompeted by the lysine residues and other alanine residues as indicated by Figure 7a. Therefore, we expect that the K4, A4, and C-terminus tend to form a tail region away from the surface. It should be noted that the surface composition of the C- and N-terminus groups are less than 0.04 (not shown). Clearly, the segment-level details are important for understanding the unique feature of polypeptide adsorption.

We present in Figure 7b the total segment distribution as a function of distance from the surface and pH. The accumulation of the polypeptide at the surface follows a bell-shape with pH in the range of 3 to 11. Unlike the acidic polypeptide, the basic polypeptide shows a noticeable presence of peptide in the following layers after the surface, particularly around pH 8. The profile

away from the surface agrees with the notion that the peptide has a tail region away from the surface which is present with K4, A4, and C-terminus groups. The weaker non-electrostatic binding results in more conformational flexibility for the polypeptide as it no longer needs to lay flat along the surface (i.e., within the square-well width) to maximize the surface attraction.

3.3 Adsorption of oligopeptide with acidic and basic residues

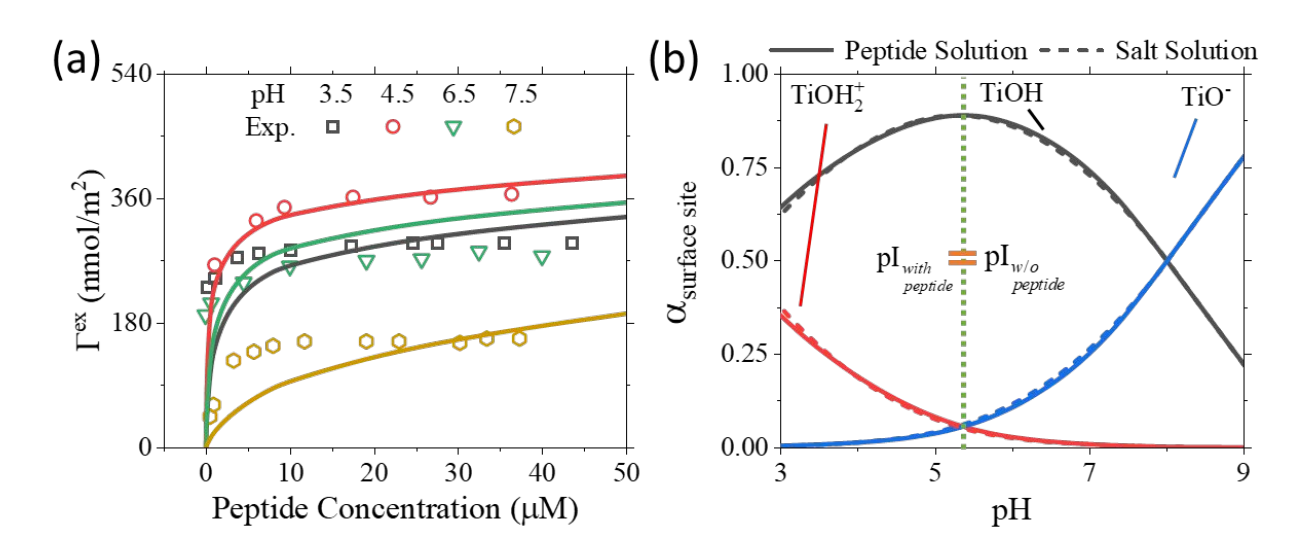


Figure 8. (a) The pH-dependence of adsorption isotherms for amphiphilic polypeptide DKDKDKDK on the titanium surface in a 100 mM potassium nitrate solution. The lines are the theoretical predictions and the symbols are from experiment⁵². (b) The fractions of different ionizable sites at the titanium surface in 100 mM KNO₃ solution with and without the polypeptide (at 50 μ M).

The last case we consider is the adsorption of polyampholyte DKDKDKDK to the titanium surface. Figure 8a shows the adsorption isotherms at different solution pH values. The alternating sequence of the polypeptide leads to attractive intrachain interactions between neighboring residues; therefore, all residues maintain full ionization in the pH range considered in this work. As a result, the polypeptide has a net charge of zero and we expect that the polypeptide adsorption

would less sensitive to the change in surface charge and pH. Indeed, we find that the polypeptide shows relatively similar adsorption for the pH 3.5, 4.5, and 6.5, but a noticeable drop in adsorption when the pH is 7.5. The latter can be explained by the reduction in the non-electrostatic binding energy due to the deprotonation of the surface sites as the surface charges more negatively. Thus, we find that the polyampholyte represents a middle ground between the strong binding by the aspartic-acid residues and the weaker binding by the lysine residues. We show the influence of the polypeptide on the surface speciation in Figure 8b. As expected from its "neutral" nature, the polypeptide has a minimal impact on the speciation of the titanium surface because it does not contribute to the net charge of the fluid.

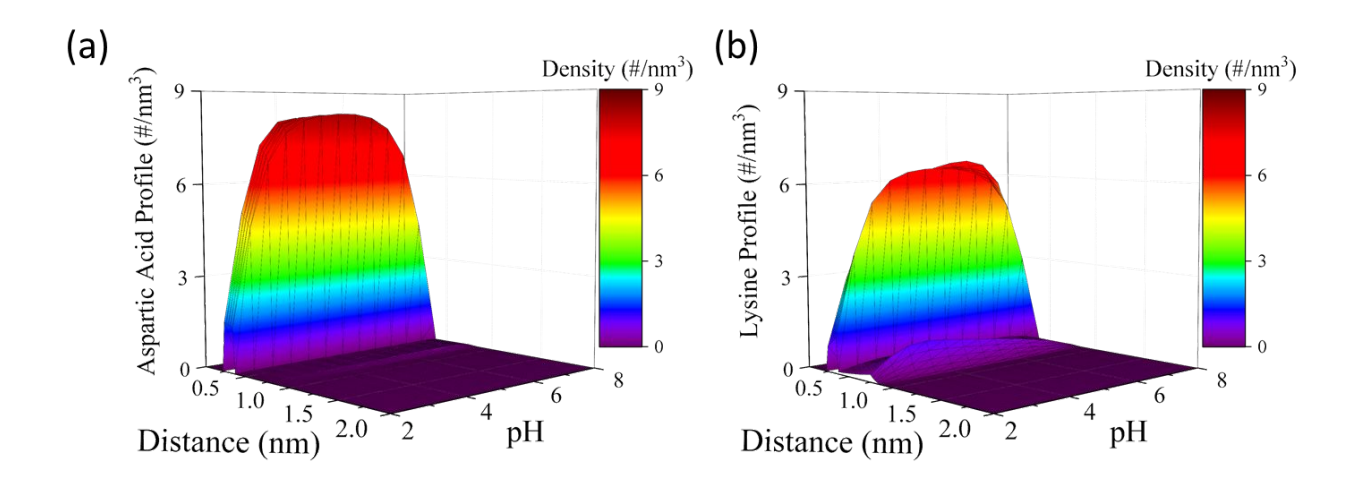


Figure 9. The segment profile for the (a) aspartic-acid residues and (b) lysine residues of the amphiphilic oligopeptide as a function of distance from the surface and solution pH. The bulk concentrations of polypeptide and KNO₃ are 50 μ M and 100 mM, respectively.

Lastly, Figure 9 shows the segment distribution as a function of distance and pH for the two different residues in the oligopeptide DKDKDKDK. The polyampholyte shows adsorption to the surface in the pH range from 2 to 8 after which the high charge of the surface leads to the counterions outcompeting the "neutral" polypeptide in the surface region. By comparing Figure

9a and 9b, we see that the aspartic-acid residues dominate the surface region and show little presence in the following layers. In contrast, lysine residues show a noticeable presence in the layer following the surface (but still within the square-well width); particularly at low pH. Since aspartic-acid residues bind strongly to the surface through the square-well potential, they maintain a relatively consistent occupancy of the surface region in the pH range that the polypeptide is adsorbed to the titanium surface. On the other hand, lysine residues do not bind as strongly to the surface and therefore are more susceptible to the variation in the surface charge. When the surface is positively charged (low pH), it is more preferable to exclude lysine residues in the surface layer. On the other hand, at high pH, the favorable electrostatic interaction between the positively charged lysine residues and negatively charged surface leads to more adsorption of lysine residues in the surface region and, therefore, the presence of lysine in the second layer is reduced. At low and high pH, the surface becomes highly charged and counterions will occupy the surface region instead of the polypeptide.

4. Conclusion

There have been substantial interests in understanding the interaction of polypeptides and proteins with inorganic surfaces due to their applications to the design of bioadhesives and the remediation of biofouling. In the present study, we have initiated a theoretical work for such possibilities by employing a coarse-grained model for polypeptides that captures their adsorption at an inorganic surface under different solution conditions. By leveraging our previous work to account for the key physics governing charge regulation and the interaction of amino acids with ionic species in aqueous solutions, we have developed a molecular theory that is able to predict the adsorption of polypeptides on inorganic surfaces driven by electrostatic binding and/or surface complexation. The thermodynamic model integrates ionization equilibrium for both polypeptide

and inorganic surfaces with the Ising density functional theory (iDFT) that facilitates an accurate description of the inhomogeneous distributions of polypeptides and ionic species near ionizable inorganic surfaces. Importantly, this model accounts for both chemical and physical interactions between polypeptides and an inorganic surface, which is key to capturing the changes in adsorption due to variation in solution conditions.

To demonstrate the effectiveness of our model, we compare the theoretical predictions directly with experimental adsorption data for different oligopeptides featuring acidic, basic, and neutral monomers on a titanium surface. We have investigated the adsorption behavior of different oligopeptides at the titanium surface in aqueous solutions that are varied in pH. We found that polypeptide adsorption typically shows a maximum in pH that is dependent upon the type of residues in the peptide. For acidic residues, the non-electrostatic surface binding makes a significant contribution to the adsorption even when the electrostatic charges of the acidic residue and the surface are of the same sign. On the other hand, a basic residue like lysine shows a much weaker dependence on non-electrostatic surface binding and the adsorption is mostly driven by electrostatic attraction from the surface. A maximum adsorption takes place at high pH where the surface sites are mostly deprotonated and as a result the non-electrostatic interaction is diminished due to the lack of hydrogen bonding sites for the carbonyl group in the backbone.

An accurate description of the charge regulation for both polypeptides and the underlying surface in a highly inhomogeneous environment plays an important role in understanding the adsorption behavior of polypeptides, particularly when the peptide sequence contains acidic and basic residues, to inorganic surfaces. The interaction between polypeptides and the surface also affects equilibrium between different charged states leading to the speciation of the polymer significantly different from that in the bulk solution. Because of the shift in speciation, the peptide

adsorbed at a highly charged surface may exist in an ionized state of opposite charge to the surface while those in the bulk solution are entirely neutral. Although the coarse-grained model to capture polypeptide adsorption employs a number of semi-empirical parameters (viz. square-well attraction energy for the monomers lysine, alanine, and aspartic acid), it provides a predictive description of thermodynamic non-idealities that are relevant to describe the environmental effects on both polypeptide adsorption and chemical equilibrium. In the future, we plan to extend this theoretical framework to describing the adsorption of flexible proteins which are of keen interest for practical applications such as in bioadhesives.

Acknowledgements

This work is financially supported by the NSF-DFG Lead Agency Activity in Chemistry and Transport in Confined Spaces under Grant No. NSF 2234013. Additional support is provided by the National Science Foundation Graduate Research Fellowship under Grant No. DGE-1326120. The computational work used resources of the National Energy Research Scientific Computing Center (NERSC), a DOE Office of Science User Facility supported by the Office of Science of the U.S. Department of Energy, under Contract DE-AC02-05CH11231.

References

- 1. Lim, Y. P.; Mohammad, A. W., Influence of pH and ionic strength during food protein ultrafiltration: Elucidation of permeate flux behavior, fouling resistance, and mechanism. *Separation Science and Technology* **2012**, *47* (3), 446-454.
- 2. Barish, J. A.; Goddard, J. M., Anti-fouling surface modified stainless steel for food processing. *Food and Bioproducts processing* **2013**, *91* (4), 352-361.
- 3. Mérian, T.; Goddard, J. M., Advances in nonfouling materials: perspectives for the food industry. *Journal of agricultural and food chemistry* **2012**, *60* (12), 2943-2957.
- 4. Waite, J. H., Mussel adhesion essential footwork. *Journal of Experimental Biology* **2017**, *220* (4), 517-530.
- 5. Stewart, R. J.; Wang, C. S.; Song, I. T.; Jones, J. P., The role of coacervation and phase transitions in the sandcastle worm adhesive system. *Advances in colloid and interface science* **2017**, *239*, 88-96.
- 6. MacEwan, S. R.; Chilkoti, A., Applications of elastin-like polypeptides in drug delivery. *Journal of Controlled Release* **2014**, *190*, 314-330.
- 7. González-Aramundiz, J. V.; Lozano, M. V.; Sousa-Herves, A.; Fernandez-Megia, E.; Csaba, N., Polypeptides and polyaminoacids in drug delivery. *Expert Opinion on Drug Delivery* **2012**, *9* (2), 183-201.

- 8. Talmadge, J. E., The pharmaceutics and delivery of therapeutic polypeptides and proteins. *Advanced drug delivery reviews* **1993**, *10* (2-3), 247-299.
- 9. Costa, D.; Savio, L.; Pradier, C.-M., Adsorption of amino acids and peptides on metal and oxide surfaces in water environment: a synthetic and prospective review. *The Journal of Physical Chemistry B* **2016**, *120* (29), 7039-7052.
- 10. Costa, D.; Garrain, P. A.; Baaden, M., Understanding small biomolecule-biomaterial interactions: A review of fundamental theoretical and experimental approaches for biomolecule interactions with inorganic surfaces. *Journal of Biomedical Materials Research Part A* **2013**, *101* (4), 1210-1222.
- 11. Petrenko, V., Evolution of phage display: from bioactive peptides to bioselective nanomaterials. *Expert opinion on drug delivery* **2008**, *5* (8), 825-836.
- 12. Ogi, H., Wireless-electrodeless quartz-crystal-microbalance biosensors for studying interactions among biomolecules: A review. *Proceedings of the Japan Academy, Series B* **2013**, *89* (9), 401-417.
- 13. Van Noort, D.; Welin-Klintström, S.; Arwin, H.; Zangooie, S.; Lundström, I.; Mandenius, C.-F., Monitoring specific interaction of low molecular weight biomolecules on oxidized porous silicon using ellipsometry. *Biosensors and Bioelectronics* **1998**, *13* (3-4), 439-449.
- 14. Nguyen, H. H.; Park, J.; Kang, S.; Kim, M., Surface plasmon resonance: a versatile technique for biosensor applications. *Sensors* **2015**, *15* (5), 10481-10510.
- 15. Landoulsi, J.; Dupres, V., Probing Peptide–Inorganic Surface Interaction at the Single Molecule Level Using Force Spectroscopy. *ChemPhysChem* **2011**, *12* (7), 1310-1316.
- 16. Maity, S.; Zanuy, D.; Razvag, Y.; Das, P.; Alemán, C.; Reches, M., Elucidating the mechanism of interaction between peptides and inorganic surfaces. *Physical Chemistry Chemical Physics* **2015**, *17* (23), 15305-15315.
- 17. Kuboyama, M.; Kato, R.; Okochi, M.; Honda, H., Screening for silver nanoparticle-binding peptides by using a peptide array. *Biochemical engineering journal* **2012**, *66*, 73-77.
- 18. Imamura, K.; Shimomura, M.; Nagai, S.; Akamatsu, M.; Nakanishi, K., Adsorption characteristics of various proteins to a titanium surface. *Journal of bioscience and bioengineering* **2008**, *106* (3), 273-278.
- 19. Lambert, J. F., Adsorption and polymerization of amino acids on mineral surfaces: a review. *Orig Life Evol Biosph* **2008**, *38* (3), 211-42.
- 20. Begonja, S.; Rodenas, L. A. G.; Borghi, E. B.; Morando, P. J., Adsorption of cysteine on TiO2 at different pH values: Surface complexes characterization by FTIR-ATR and Langmuir isotherms analysis. *Colloids and Surfaces A: Physicochemical and Engineering Aspects* **2012**, *403*, 114-120.
- 21. El Shafei, G. M. S.; Moussa, N. A., Adsorption of Some Essential Amino Acids on Hydroxyapatite. *Journal of Colloid and Interface Science* **2001**, *238* (1), 160-166.
- 22. Imamura, K.; Mimura, T.; Okamoto, M.; Sakiyama, T.; Nakanishi, K., Adsorption Behavior of Amino Acids on a Stainless Steel Surface. *Journal of Colloid and Interface Science* **2000**, *229* (1), 237-246.
- 23. O'Connor, A. J.; Hokura, A.; Kisler, J. M.; Shimazu, S.; Stevens, G. W.; Komatsu, Y., Amino acid adsorption onto mesoporous silica molecular sieves. *Separation and Purification Technology* **2006**, *48* (2), 197-201.
- 24. Gama, M. d. S.; Barreto, A. G.; Tavares, F. W., The binding interaction of protein on a charged surface using Poisson–Boltzmann equation: lysozyme adsorption onto SBA-15. *Adsorption* **2021**, *27* (7), 1137-1148.
- 25. Boubeta, F. M.; Soler-Illia, G. J. A. A.; Tagliazucchi, M., Electrostatically Driven Protein Adsorption: Charge Patches versus Charge Regulation. *Langmuir* **2018**, *34* (51), 15727-15738.
- 26. Biesheuvel, P. M.; Leermakers, F. A. M.; Stuart, M. A. C., Self-consistent field theory of protein adsorption in a non-Gaussian polyelectrolyte brush. *Physical Review E* **2006**, *73* (1), 011802.
- 27. Kurut, A.; Henriques, J.; Forsman, J.; Skepö, M.; Lund, M., Role of histidine for charge regulation of unstructured peptides at interfaces and in bulk. *Proteins: Structure, Function, and Bioinformatics* **2014**, *82* (4), 657-667.

- 28. Biesheuvel, P. M.; van der Veen, M.; Norde, W., A Modified Poisson–Boltzmann Model Including Charge Regulation for the Adsorption of Ionizable Polyelectrolytes to Charged Interfaces, Applied to Lysozyme Adsorption on Silica. *The Journal of Physical Chemistry B* **2005**, *109* (9), 4172-4180.
- 29. Leermakers, F. A. M.; Atkinson, P. J.; Dickinson, E.; Horne, D. S., Self-Consistent-Field Modeling of Adsorbed β -Casein: Effects of pH and Ionic Strength on Surface Coverage and Density Profile. *Journal of Colloid and Interface Science* **1996**, *178* (2), 681-693.
- 30. Dickinson, E.; S. Horne, D.; J. Pinfield, V.; A. M. Leermakers, F., Self-consistent-field modelling of casein adsorption Comparison of results for $\alpha s1$ -casein and β -casein. *Journal of the Chemical Society, Faraday Transactions* **1997**, *93* (3), 425-432.
- 31. Verde, A. V.; Acres, J. M.; Maranas, J. K., Investigating the specificity of peptide adsorption on gold using molecular dynamics simulations. *Biomacromolecules* **2009**, *10* (8), 2118-2128.
- 32. Xie, Y.; Liu, M.; Zhou, J., Molecular dynamics simulations of peptide adsorption on self-assembled monolayers. *Applied Surface Science* **2012**, *258* (20), 8153-8159.
- 33. Wei, S.; Knotts IV, T. A., A coarse grain model for protein-surface interactions. *The Journal of chemical physics* **2013**, *139* (9), 09B631 1.
- 34. Kmiecik, S.; Gront, D.; Kolinski, M.; Wieteska, L.; Dawid, A. E.; Kolinski, A., Coarse-grained protein models and their applications. *Chemical reviews* **2016**, *116* (14), 7898-7936.
- 35. Hyltegren, K.; Nylander, T.; Lund, M.; Skepö, M., Adsorption of the intrinsically disordered saliva protein histatin 5 to silica surfaces. A Monte Carlo simulation and ellipsometry study. *Journal of Colloid and Interface Science* **2016**, *467*, 280-290.
- 36. Qiu, R.; Xiao, J.; Chen, X. D., Further understanding of the biased diffusion for peptide adsorption on uncharged solid surfaces that strongly interact with water molecules. *Colloids and Surfaces A: Physicochemical and Engineering Aspects* **2017**, *518*, 197-207.
- 37. Grünewald, F.; Souza, P. C. T.; Abdizadeh, H.; Barnoud, J.; de Vries, A. H.; Marrink, S. J., Titratable Martini model for constant pH simulations. *The Journal of Chemical Physics* **2020**, *153* (2), 024118.
- 38. Longo, G. S.; Olvera de la Cruz, M.; Szleifer, I., Equilibrium Adsorption of Hexahistidine on pH-Responsive Hydrogel Nanofilms. *Langmuir* **2014**, *30* (50), 15335-15344.
- 39. Wagner, A. M.; Gran, M. P.; Peppas, N. A., Designing the new generation of intelligent biocompatible carriers for protein and peptide delivery. *Acta pharmaceutica sinica B* **2018**, *8* (2), 147-164.
- 40. Dai, X.; Chen, Y., Computational Biomaterials: Computational Simulations for Biomedicine. *Advanced Materials* **2022**, 2204798.
- 41. Gallegos, A.; Wu, J., Molecular thermodynamics for amino-acid adsorption at inorganic surfaces. *AIChE Journal* **2021**, e17432.
- 42. Ong, G. M. C.; Gallegos, A.; Wu, J., Modeling Surface Charge Regulation of Colloidal Particles in Aqueous Solutions. *Langmuir* **2020**.
- 43. Gallegos, A.; Ong, G. M. C.; Wu, J., Ising density functional theory for weak polyelectrolytes with strong coupling of ionization and intrachain correlations. *The Journal of Chemical Physics* **2021**, *155* (24), 241102.
- 44. Gallegos, A.; Wu, J., Charge Regulation of Natural Amino Acids in Aqueous Solutions. *Journal of Chemical & Engineering Data* **2020**.
- 45. Jin, Z.; Tang, Y.; Wu, J., A perturbative density functional theory for square-well fluids. *The Journal of Chemical Physics* **2011**, *134* (17), 174702.
- 46. Spruijt, E.; Biesheuvel, P. M.; de Vos, W. M., Adsorption of charged and neutral polymer chains on silica surfaces: The role of electrostatics, volume exclusion, and hydrogen bonding. *Physical Review E* **2015**, *91* (1), 012601.
- 47. Loux, N. T., Extending the diffuse layer model of surface acidity behaviour: III. Estimating bound site activity coefficients. *Chemical Speciation & Bioavailability* **2009**, *21* (4), 233-244.

- 48. Wertheim, M., Thermodynamic perturbation theory of polymerization. *The Journal of chemical physics* **1987**, *87* (12), 7323-7331.
- 49. Yu, Y.-X.; Wu, J., Structures of hard-sphere fluids from a modified fundamental-measure theory. *The Journal of Chemical Physics* **2002**, *117* (22), 10156-10164.
- 50. Voukadinova, A.; Valiskó, M.; Gillespie, D., Assessing the accuracy of three classical density functional theories of the electrical double layer. *Physical Review E* **2018**, *98* (1), 012116.
- 51. Gallegos, A.; Ong, G. M. C.; Wu, J., Thermodynamic non-ideality in charge regulation of weak polyelectrolytes. *Soft Matter* **2021**.
- 52. Imamura, K.; Kawasaki, Y.; Nagayasu, T.; Sakiyama, T.; Nakanishi, K., Adsorption characteristics of oligopeptides composed of acidic and basic amino acids on titanium surface. *Journal of Bioscience and Bioengineering* **2007**, *103* (1), 7-12.
- 53. Zhuravlev, L., Concentration of hydroxyl groups on the surface of amorphous silicas. *Langmuir* **1987**, *3* (3), 316-318.

TOC Graphic

